

Fluid Mechanics of the Human Eye: Aqueous Humour Flow in the Anterior Chamber

A. D. Fitt*, G. Gonzalez

School of Mathematics, University of Southampton, Southampton SO17 1BJ, UK

Received: 7 July 2004 / Accepted: 27 January 2005
© Society for Mathematical Biology 2006

Abstract We consider and compare the various different kinds of flow that may take place in the anterior chamber of a human eye. The physical mechanisms responsible for causing such flows may be classified as follows: (i) buoyancy-driven flow arising from the temperature difference between the anterior surface of the cornea and the iris, (ii) flow generated by the aqueous production of the ciliary body, (iii) flow generated by the interaction between buoyancy and gravity while sleeping while sleeping in a face-up position, (iv) flow generated by phakodonesis (lens tremor), (v) flow generated by Rapid Eye Movement (REM) during sleep. Each flow is studied using a traditional fluid mechanics/asymptotic analysis approach. We also assess the veracity of a hypothesis that was recently advanced [see Maurice, D.M., 1998. The Von Sallman Lecture 1996: An ophthalmological explanation of REM sleep. *Exp. Eye. Res.* 66, 139–145, for details] to suggest that, contrary to previous opinion, the purpose of REM during sleep is to ensure corneal respiration in the absence of the buoyant mixing that routinely takes place due to (i) above during waking conditions.

Keywords Aqueous humour circulation · Anterior chamber flow · Fluid mechanics · Convective flow · REM sleep · Phakodonesis

1. Introduction

It has long been known that a number of distinct mechanisms can act to cause the motion of aqueous humour in the anterior chamber of a human eye. Normally patients are unaware that any such flow occurs, for the transparency of the aqueous gives no hint of the flow that is occurring. Flow in the anterior chamber becomes much more important (a) when particulate matter (red/white blood cells or pigment particles) is present (see Section 2 below) and (b) when it is desired to use the flow for a clinical purpose (for example, the distribution of drugs within the anterior chamber, Wyatt, 1996).

*Corresponding author.

E-mail addresses: adf@maths.soton.ac.uk (A. D. Fitt), ggc@maths.soton.ac.uk (G. Gonzalez).

Table 1 Standard parameter values for an adult human eye

Physical quantity	Typical value
Radius of anterior chamber ^a a (m)	5.5×10^{-3}
Total width of anterior chamber ^a l (m)	11×10^{-3}
Coefficient of linear expansion of aqueous humour ^b α (/K)	3.0×10^{-4}
Gravitational acceleration g (m/s^2)	9.8×10^0
Height of anterior chamber ^a h_0 (m)	2.75×10^{-3}
Dynamic viscosity μ of aqueous humour ^{b,c} (Pa s)	1.0×10^{-3}
Density ρ_0 of aqueous humour ^c (kg/m^3)	1.0×10^3

^aBron et al. (1997).

^bBatchelor (1985).

^cFatt and Weissman, (1992).

The various mechanisms that cause flow of aqueous inside the anterior chamber, namely temperature differences, secretory flow from the ciliary body through the pupil aperture and ultimately to the trabecular meshwork, gravity, and movement of the eye itself will be considered in turn, using classical fluid mechanics and asymptotic analysis. In each case the importance of the flow thus produced will be assessed. Throughout, we shall use typical parameter values for a normal adult human eye. These are summarised in Table 1, where aqueous humour is considered to have properties very similar to water (Fatt and Weissman, 1992). (In reality the primary source of aqueous humour is the ultrafiltration of blood plasma.) We shall also assume for simplicity that the corneal shape is given by a simple known function relating its height to position: using more accurate measured profiles would cause no difficulties other than a complication (and consequent obfuscation) of the algebra involved.

2. Buoyant flow driven by temperature differences

It has long been acknowledged that aqueous humour in the anterior chamber can circulate under the action of buoyancy-driven currents. The driving mechanism for these currents is the temperature difference between the anterior surface of the cornea (which, under normal waking conditions is exposed to ambient conditions) and the iris (which is maintained essentially at body temperature). The existence of buoyancy-driven anterior chamber flow was demonstrated experimentally in Wyatt (1996) where changes in aqueous circulation were promoted by the application of hot or cold packs to the closed lids of a human eye.

The fluid mechanics underlying this phenomenon was investigated theoretically in Canning et al. (2002), where it was shown that the “lubrication theory” limit of the Navier–Stokes equations was appropriate. Using the Boussinesq approximation for the buoyancy, it was shown that, to leading order, the flow satisfies the partial differential equations

$$-\frac{P_x}{\rho_0} + \nu u_{zz} + g(1 - \alpha(T - T_0)) = 0 \quad (1)$$

$$-\frac{p_y}{\rho_0} + \nu v_{zz} = 0 \tag{2}$$

$$p_z = 0 \tag{3}$$

$$u_x + v_y + w_z = 0 \tag{4}$$

$$T_{zz} = 0 \tag{5}$$

subject to the boundary conditions

$$u = v = 0, \quad w = w_0(x, y), \quad T = T_1 \quad \text{on} \quad z = 0, \tag{6}$$

$$u = v = w = 0, \quad T = T_0 \quad \text{on} \quad z = h(x, y). \tag{7}$$

In (1)–(7) the fluid velocity is denoted by $\mathbf{q} = (u, v, w)^T$ and the coordinate system (x, y, z) is as shown in Fig. 1. The temperature and pressure of the aqueous are denoted by T and p respectively, the posterior surface of the cornea is assumed to be at $z = h(x, y)$, and $w = w_0(x, y)$ specifies the flow (if any) through the pupil aperture. T_0 and T_1 denote the temperatures of the posterior surface of the cornea and the anterior surface of the iris respectively, and ν, ρ_0 and α denote respectively the kinematic viscosity, fluid density when $T = T_0$ and coefficient of linear expansion of the aqueous.

Under the simplest assumptions (namely no flow through the pupil aperture so that $w_0 = 0$, gravity acting along the positive x -axis and hydrostatic pressure) we find that $v = 0$, so that flow takes place in two-dimensional vertical (x, z) -slices of the anterior chamber. The solution in this case is given by

$$p = p_a + g\rho_0(x + a)(2 - \alpha(T_1 - T_0))/2 \tag{8}$$

$$T = T_1 + \frac{z}{h}(T_0 - T_1) \tag{9}$$

$$\psi = -\frac{(T_1 - T_0)g\alpha z^2(z - h)^2}{24\nu h} \tag{10}$$

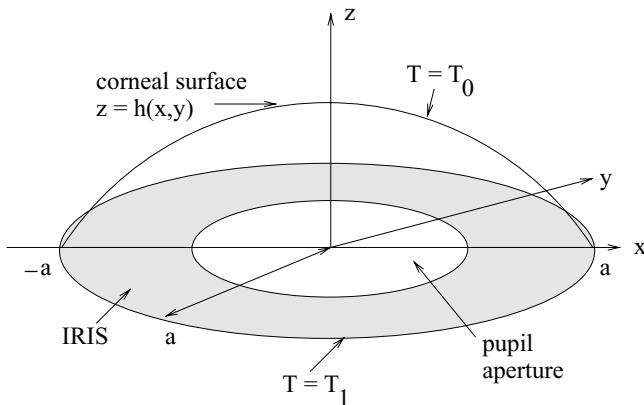


Fig. 1 Schematic diagram and nomenclature of anterior chamber of a human eye.

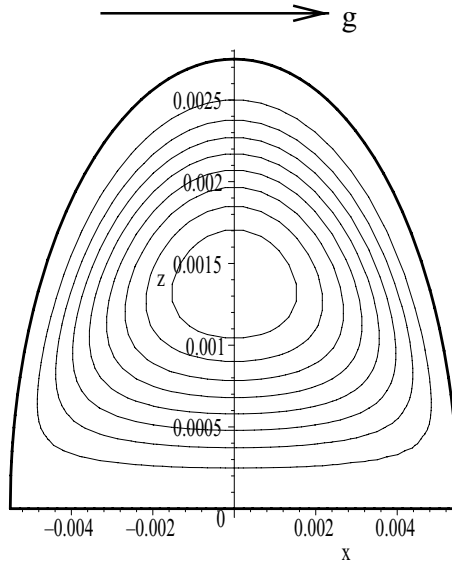


Fig. 2 Streamlines for buoyancy-driven flow in anterior chamber in the slice $y = 0$: Parameter values as in Table 1 with $T_1 - T_0 = 2^\circ\text{C}$ and $h(x, y) = h_0\sqrt{1 - r^2/a^2}$.

where p_a is the ambient pressure and the stream function $\psi(x, z)$ is defined by $u = \psi_z$, $w = -\psi_x$. Streamlines of this flow in the plane $y = 0$ for the values given in Table 1 with $h(x, y) = h_0(1 - r^2/a^2)^{1/2}$ are shown in Fig. 2. (Note that here and henceforth the vertical axis is stretched to allow the flow details to be more easily visible.)

Using typical parameter values as given in Table 1, we find that a typical maximum flow speed in the anterior chamber is given by

$$u_{\max} \sim (T_1 - T_0) \times 1.98 \times 10^{-4} \text{ m s}^{-1} \text{ K}^{-1}.$$

From this we conclude that, even for relatively small temperature differences, aqueous humour circulation speeds of order 0.1 mm/s may be expected. The analysis contained in subsequent sections will confirm that buoyant flow of this sort provides by far the most powerful force to drive flow in the anterior chamber, producing flow speeds that are an order of magnitude greater than any other mechanism.

Many other interesting conclusions may be drawn from the details of such flow. For example, the shear stress may be calculated to determine whether or not the flow is strong enough to detach pigment particles from the iris. Comparison with the experimental values of Gerlach et al. (1997) and Vankooten et al. (1994) soon show that the flow is not nearly powerful enough to cause such effects, so that buoyancy-driven flow in the anterior chamber cannot be solely responsible (as has previously been suggested) for the presence of pigment particles in the anterior chamber. It is also possible to propose various other models, more sophisticated than that used here, for the heat transfer across the cornea, but such developments

make only minor differences to both the quantitative and qualitative details of the flow.

Once the flow is known, it is a simple matter to include particles in the analysis. This is done in detail in [Canning et al. \(2002\)](#). In this manner predictions may be made of hyphemas (patterns formed by red blood cells in the anterior chamber) hypopyons (formed by white blood cells) and Krukenberg spindles (composed of pigment particles). The theory may also be used to predict how a hyphema may be disrupted by the application of a cold patch to the eye.

3. Aqueous flow through the pupil aperture

When a patient has been asleep for a period of more than a few minutes, it seems reasonable to assume that the generous supply of blood vessels in the eyelid may render the temperature in the anterior chamber close to uniform and therefore greatly reduce the strength of flow predicted by (8)–(10). In the absence of a dominant buoyancy-driven flow the only remaining mechanism for causing flow in a stationary eye is the passage of fresh aqueous through the pupil aperture. The resulting flow may easily be predicted using the thin-layer theory outlined in [Canning et al. \(2002\)](#). Assuming cylindrical symmetry so that the flow depends only on z and the radial direction r , the equations of motion are

$$P_r = \mu u_{zz}, \quad P_z = 0, \quad \frac{1}{r}(ru)_r + w_z = 0.$$

Here the hydrostatic pressure has been subtracted so that $p = -\rho_0gz + P(r)$ and the fluid velocity is now $\mathbf{q} = u\hat{\mathbf{e}}_r + w\hat{\mathbf{e}}_z$ where $\hat{\mathbf{e}}_r$ and $\hat{\mathbf{e}}_z$ are unit vectors in the r and z directions respectively.

The boundary conditions for the flow are that both u and w are zero on the corneal surface $z = h(r)$, u is zero on $z = 0$, and that $w = w_0(r)$ on $z = 0$. Solving, we find that

$$u = \frac{zP_r}{2\mu}(z - h(r)), \quad w = \frac{z^2}{12\mu r}[(3h - 2z)(rP_r)_r + 3rh_rP_r] + w_0(r)$$

where $P(r)$ satisfies

$$(rh^3P_r)_r = -12\mu r w_0.$$

Many possible examples may now be examined; one of the simplest consists of taking

$$h = h_0(1 - r^2/a^2)^{1/2}, \quad w_0 = A_4(r^2 - a^2)(r^2 - a^2/3) \tag{11}$$

whence

$$P = \frac{2A_4\mu a^3}{3h_0^3}(a^2 - r^2)^{3/2}. \tag{12}$$

Here A_i is a constant that characterises the strength of the flow. This choice for w_0 assumes that the pupil aperture has radius¹ $a/\sqrt{3}$ through which the flow has a parabolic velocity profile, and that outflow takes place over the rest of the iris (in reality of course outflow takes place only very near the angle).

The simplicity of (11) will be exploited in Section 3.1, but for the present we will use the more realistic choice

$$w_0 = K_1(b^2 - r^2)H(b - r) - K_2H(r - (a - \delta)) \quad (13)$$

where H is a Heaviside function, $b = ka$ is the radius of the pupil aperture ($k < 1$) and K_1 , K_2 and δ are constants. Now flow with a parabolic velocity profile enters through the pupil aperture $0 \leq r \leq b$ and the flow exits as a plug flow over the region $a - \delta \leq r \leq a$ at the limbus (the visible junction between the transparent cornea and the white-coloured sclera). Choosing

$$K_2 = \frac{a^4 k^4 K_1}{2\delta(2a - \delta)}$$

ensures that mass is conserved in the anterior chamber, and we find further that the mass flow into the anterior chamber is $K_1 b^4/4$ and

$$\begin{aligned} \psi = \frac{(2z + h)(z - h)^2}{4h^3} [& K_1 r^2 (r^2 - 2b^2) - K_1 (r^2 - b^2)^2 H(r - b) \\ & + 2K_2 (r^2 - (a - \delta)^2) H(r - a + \delta)] \end{aligned} \quad (14)$$

and

$$P_r = \frac{12\mu\psi}{r(2z + h)(z - h)^2}.$$

As far as the constant K_1 is concerned, typical values for the mass flow through the pupil aperture are given in (Brubaker, 1996), who suggests that the flow of aqueous is diurnal, having a value of $1.23 \pm 0.41 \mu\text{l}/\text{min}$ between the hours of midnight and 06.00. A value of $1.23 \mu\text{l}/\text{min}$ thus corresponds to taking $K_1 = 8.603 \times 10^{10} \mu\text{l}/\text{min}$. Using the standard values given in Table 1 with $k = 1/2$, we find that the streamlines are as shown in Fig. 3. The maximum speed of the flow is $7.5 \times 10^{-6} \text{m/s}$, which compares well with the order of magnitude estimate in Maurice (1998) of $0.1 \text{mm}/\text{min} \sim 1.7 \times 10^{-6} \text{m/s}$.

3.1. Combined buoyant and secretory flow

Finally, it is worth noting that it is also possible to examine a case where the buoyant convection is small enough just to balance the secretory flow through the pupil

¹Pupil aperture radius normally varies between about 1 and 3 mm, the latter figure being achieved by young patients in essentially dark surroundings.

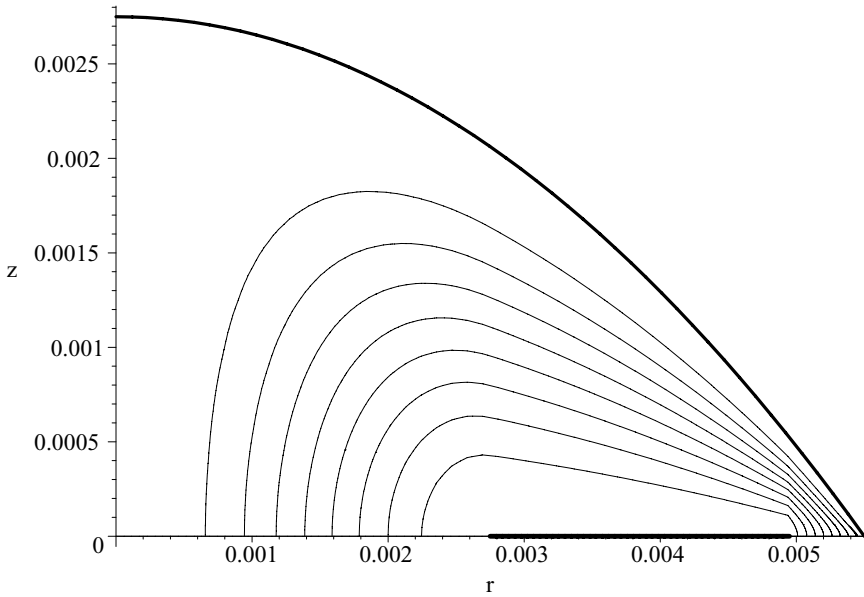


Fig. 3 Streamlines of secretory flow described by (14) for standard values from Table 1 with $k = 1/2$, $\delta = a/10$ and $K_1 = 8.603 \times 10^{10} \mu\text{l}/\text{min}$. Corneal shape given by $h(r) = h_0(1 - r^2/a^2)$, w_0 as given by (13).

aperture. When the patient adopts a vertical position so that gravity acts in the direction of the x -axis, the flow streamlines become fully three-dimensional and very complicated (for more details see [Canning et al. , 2002](#)).

4. Buoyancy-driven flow during sleep

When a patient sleeps in a face-up position gravity acts vertically downwards from the cornea to the iris. [Maurice \(1998\)](#) notes that it may be possible that the supply of blood in the eyelids is not sufficient to warm the corneal surface to body temperature during sleep, so that a small temperature difference between the posterior surface of the cornea and the iris and thus a residual thermal circulation might persist. This will drive drive a buoyant flow different in character from that described in Section 2. Ignoring secretory flow from the ciliary body, we again assume axisymmetric flow with fluid velocity $\mathbf{q} = u\hat{\mathbf{e}}_r + w\hat{\mathbf{e}}_z$. Under the standard lubrication theory approximation and using the same notation as in the sections above, the equations to be solved are now

$$p_r = \mu u_{zz}, \quad \frac{p_z}{\rho_0} = -g(1 - \alpha(T - T_0)), \quad T_{zz} = 0, \quad \frac{1}{r}(ru)_r + w_z = 0$$

with boundary conditions $u(r, 0) = u(r, h(r)) = w(r, 0) = w(r, h(r)) = 0$, and $T(r, 0) = T_1$, $T(r, h(r)) = T_0$. Defining a stream function $\psi(z, r)$ by $u = \psi_z/r$, $w =$

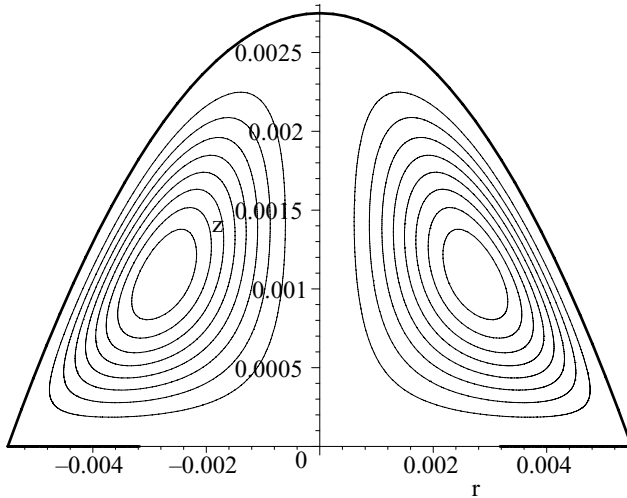


Fig. 4 Streamlines for flow produced by prone patient sleeping face-up in the absence of secretory flow ($T_0 - T_1 = 0.1^\circ\text{C}$).

$-\psi_r/r$ and using the condition that

$$\int_0^{h(r)} \left(\frac{1}{r}(ru)_r + w_z \right) dz = \frac{\partial}{\partial z}(\psi(r, h(r)) - \psi(r, 0)) = 0$$

some elementary calculations show that

$$\psi = \frac{\rho_0 g \alpha r z^2 h_r (z + 2h)(z - h)^2 (T_1 - T_0)}{120 \mu h^2}.$$

$$u = \frac{g \rho_0 h_r \alpha z (h - z)(5z^2 + 5zh - 4h^2)(T_0 - T_1)}{120 \mu h^2}$$

$$p = p_a - \rho_0 g z + \frac{\rho_0 g \alpha (3h^2 - 20zh + 10z^2)(T_0 - T_1)}{20h}$$

$$T = T_1 + \frac{z}{h}(T_0 - T_1).$$

Streamlines for the flow are shown in Fig. 4, assuming a temperature difference of 0.1°C , using values from Table 1 and now taking $h = h_0(1 - r^2/a^2)$. The flow is of a toroidal nature, the maximum speed of the flow scaling with the temperature difference. When $T_0 - T_1 = 0.1^\circ\text{C}$, the maximum speed attained by the flow is 3×10^{-6} m/s, indicating that the flow produced by this mechanism is relatively weak.

5. Flow due to phakodensis

The term “phakodensis” is used to refer to the vibration of the lens of a human eye as the head or eye moves. The lens is supported by the suspensory ligaments,

which may be thought of as being equivalent to elastic pulleys. When focusing is required, the suspensory ligaments exert a tension that changes the shape of the lens. The lens itself (one of the few parts of the human body that continues to grow from birth to death) may be thought of as a deformable bag that contains a clear protein gel. The ability of the lens to change shape under the influence of the suspensory ligaments is essential for accurate vision: the hardening of the lens with age is the primary reason why large percentages of the population who have hitherto enjoyed perfect sight develop presbyopia in middle age and require spectacles.

From a clinical point of view, any form of enhanced phakodonesis is regarded as undesirable, for it indicates weaknesses in the collagen structure of the suspensory ligaments and the zonules (the hundreds of string like fibres that hold the lens suspended in position and enable it to change shape to focus on distant or near objects). Noticeable phakodonesis may be reported, for example, in conditions such as Marfan’s syndrome (an inherited disorder of the connective tissues).

As far as the fluid mechanics of the anterior chamber are concerned, our interest in phakodonesis centres on the fact that movement of the lens acts to pump fluid through the pupil aperture. We have not been able to locate any quantitative or detailed measurements of lens movement due to phakodonesis in extant literature. We will therefore not consider the fluid mechanical details of how the lens interacts with flow behind the iris, but rather take the simpler approach of assuming (i) that the pumping speed w_0 caused by the lens movement is a known function, (ii) that this function is sinusoidal in nature (because any simple model of lens motion is likely to be based on linear springs) and (iii) that no other flow mechanisms (buoyancy, secretory flow drainage, etc.) are present so that the total net inflow/outflow to the anterior chamber is zero at all times.

Under these assumptions we proceed once again using lubrication theory. In contrast to the flows that have so far been considered in this study, however, the nature of the flow produced by the lens movement means that the flow is now not only unsteady but also can no longer be assumed to be a function simply of r and z alone. The governing equations are

$$P_r = \mu u_{zz}, \quad \frac{1}{r} P_\theta = \mu v_{zz}, \quad P_z = 0, \tag{15}$$

$$\frac{1}{r} (ru)_r + \frac{v_\theta}{r} + w_z = 0, \tag{16}$$

with velocity boundary conditions $u = v = w = 0$, on the posterior surface of the cornea $z = h(r)$ and $u = v = 0$, $w = w_0(r, \theta, t)$ on $z = 0$. Solving (15) and (16), we find that the pressure P is a function of r, θ and t only and

$$u = \frac{P_r}{2\mu} z(z-h), \quad v = \frac{P_\theta}{2\mu r} z(z-h),$$

$$w = w_0(r, \theta, t) + \frac{z^2}{4\mu} P_r h_r + \frac{1}{2\mu r^2} \left[\frac{z^2 h}{2} - \frac{z^3}{3} \right] [P_{\theta\theta} + r(r P_r)],$$

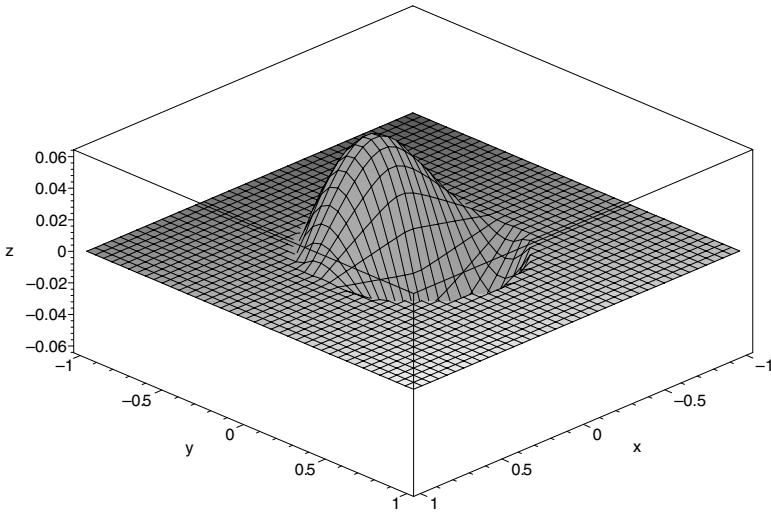


Fig. 5 Pumping velocity profile $w_0(r, \theta, t)$ as given by (18) and (19) at $t = 0$ for phakodensis-driven flow.

the boundary conditions being satisfied so long as the pressure satisfies

$$\frac{1}{r}(rh^3 P_r)_r + \frac{1}{r^2}(h^3 P_\theta)_\theta = -12\mu w_0(r, \theta, t). \tag{17}$$

Let us now assume that

$$P = p(r) \sin \theta \cos \omega t, \quad w_0 = \Omega(r) \sin \theta \cos \omega t \tag{18}$$

where ω is the frequency of the pumping. Time-dependent pumping thus takes place as the lens oscillates about the axis $\{\theta = 0\} \cup \{\theta = \pi\}$, the two sectors of the lens acting to force fluid both into and out of the anterior chamber. If we now further choose

$$\Omega(r) = Wr(r - b)H(b - r) \tag{19}$$

where b is the radius of the pupil aperture and W (dimensions $(\text{ms})^{-1}$) is a constant that characterises the strength of the pumping, then the amount of fluid entering (and also leaving) the anterior chamber at any instant is $(Wb^4 \cos \omega t/6) \text{ m}^3/\text{s}$. and the flow into and out of the anterior chamber takes place as shown in Fig. 5.

Once again assuming a simple corneal shape profile, we now set $h(r) = h_0(1 - r^2/a^2)$. Now (17) becomes the ordinary differential equation

$$r^2(a^2 - r^2)^3 p_{rr} + r(a^2 - 7r^2)(a^2 - r^2)^2 p_r - (a^2 - r^2)^3 p + \frac{12\mu Wa^6}{h_0^3} r^3(r - b)H(b - r) = 0, \tag{20}$$

which may be solved in closed form in terms of Barnes' extended hypergeometric functions ${}_2F_1$ (see for example, Abramowitz and Stegun, 1972). For practical purposes the details of the particular integral term are so unwieldy that for flow visualisation purposes it is simpler to solve (20) numerically, and this is how we shall proceed below. This may be done using any standard method, but some care must be taken over the boundary conditions. Near $r = 0$, (20) behaves as

$$r^2 p_{rr} + r p_r - p = \frac{12Wr^3 b\mu}{h_0^3}$$

which has solution $p \sim Ar + \frac{B}{r} + 3Wr^3 b\mu/2h_0^3$ ($r \sim 0$) where A and B are arbitrary constants, so since the pressure must be finite to match with the pupil aperture flow at $r = 0$ we must impose $p(0) = 0$. A similar analysis near $r = a$ shows that

$$(a - r)^3 p_{rr} - 3(a - r)^2 p_r - \frac{(a - r)^3}{a^2} p = 0$$

so that p has the Bessel function solution

$$p \sim \frac{\tilde{A}I_1\left(\frac{a-r}{a}\right) + \tilde{B}K_1\left(\frac{a-r}{a}\right)}{a - r} \quad (r \sim a)$$

where \tilde{A} and \tilde{B} are arbitrary constants. The pressure is thus finite at $r = a$ only when \tilde{B} is chosen to be zero. Accordingly, when (20) is solved numerically using an initial value scheme, we must impose $p(0) = 0$ and choose $p_r(0)$ so that the pressure is finite at $r = a$. Numerically this may easily be accomplished, and the function $p(r)$ may be determined. The resulting flow is unsteady and fully three-dimensional, but since now

$$v = \frac{P}{2\mu r} z(z - h) \cos \theta \cos \omega t$$

the azimuthal speed v is zero when $\theta = \pi/2$ or $3\pi/2$. Figure 6 shows (u, w) velocity vectors in the plane $\theta = 3\pi/2$ for values as given in Table 1 with $b = 2.5$ mm and $W = 10.42$, a value that corresponds to an amount $4.0 \mu\text{l}/\text{min}$ entering and leaving the anterior chamber at each instant. We note that the aqueous is disturbed primarily only in the region above the pupil aperture, and little flow takes place in the rest of the chamber. This qualitative picture of the flow is confirmed by Fig. 7 which shows contours of the flow speed $\sqrt{u^2 + w^2}$ for the same data used in Fig. 6.

As noted earlier, the flow is three-dimensional and unsteady. It is unusual to be able write down solutions for such flows in closed form, and the streamlines are of great interest, showing a ‘‘pumping’’ flow above the moving lens and a toroidal-type vortex nearer to the limbus. As usual, the three-dimensionality makes the flow hard to display on a two-dimensional page. However, flow animations that can be rotated in real time and viewed from many different angles may easily be created, revealing the complicated nature of the fluid motion. Realistically, however, the

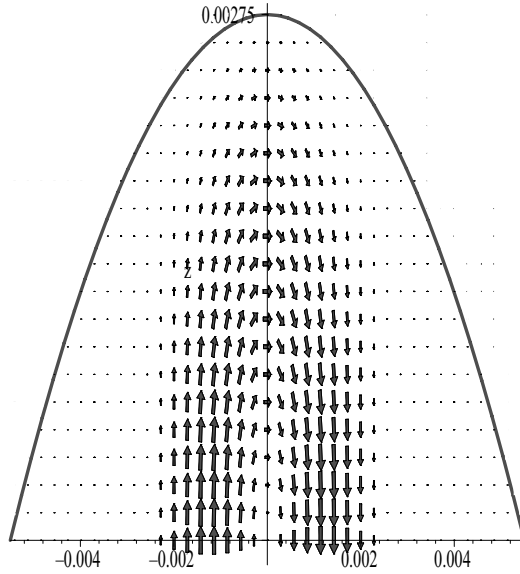


Fig. 6 Velocity $((u, w))$ -vectors in the plane $\theta = \pi/2, \theta = 3\pi/2$ for anterior chamber flow driven by phakodensitis with values as in Table 1 and $b = 2.5$ mm, $W = 10.42$ (ms) $^{-1}$, $t = 0$ and w_0 given by (18).

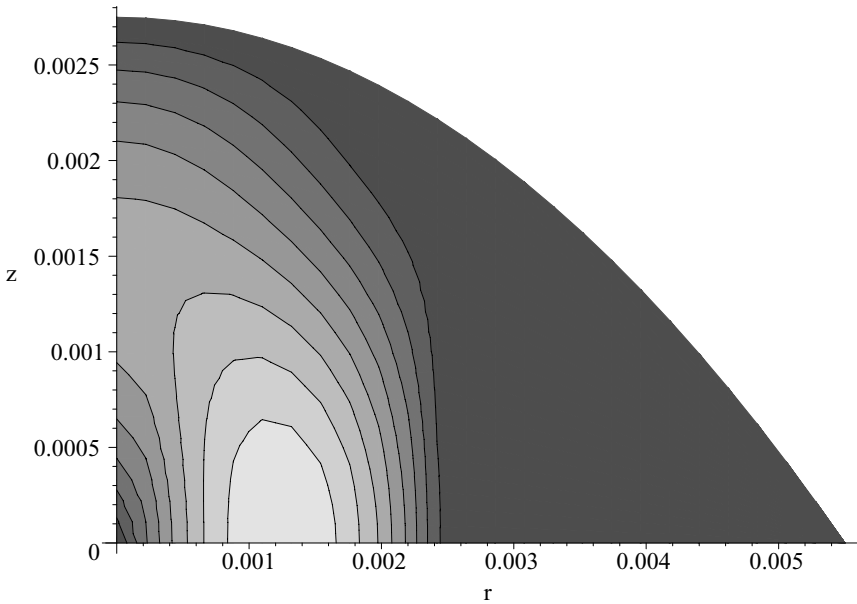


Fig. 7 Contours of flow speed $\sqrt{u^2 + w^2}$ for anterior chamber flow driven by phakodensitis (parameter values identical to Fig. 6—light regions represent larger speeds).

solutions in this section must retain a partly speculative nature until detailed experimental measurements of phakodensis have been carried out. In particular, the frequency of lens motion during phakodensis appears to remain completely unaddressed in medical literature, so that it is almost impossible to be certain that inertial effects may be ignored.

6. The limitations of lubrication theory

In all of the flows that have been examined thus far it has been assumed that the lubrication theory limit of fluid mechanics may be invoked. Some discussion of this supposition is now apposite. As far as the Navier–Stokes equations are concerned, the validity of lubrication theory is assured so long as both of the quantities ϵ (the aspect ratio) and the reduced Reynolds number $\epsilon^2 Re$ are much less than one. As explained above (see Table 1), for a typical human eye the aspect ratio (height/width) is $h_0/L = 2.75/11 = 1/4$, while an upper bound for the reduced Reynolds number $\epsilon^2 Re$ is given (for buoyancy-driven flow) by

$$\epsilon^2 Re = \frac{LU}{4^2\nu} \sim \frac{(11 \times 10^{-3})(1 \times 10^{-4})}{4^2 10^{-6}} = \frac{11}{160} = 0.06875.$$

The further assumption that (5) accurately determines the temperature requires that the reduced Peclet number $\epsilon^2 Re Pr$ should be much smaller than unity. Using a specific heat $c_p = 4200 \text{ J/kg K}$ and a thermal conductivity $k = 0.57 \text{ W/mK}$ an upper bound for this quantity is given by

$$\epsilon^2 Re Pr = \frac{11\rho_0\nu c_p}{80k} \sim 0.5$$

Since both the aspect ratio and the reduced Reynolds number $\epsilon^2 Re$ are undeniably “small,” we conclude that the lubrication theory limit is valid for the flow: for the heat transfer part of the problem, however, it could be argued *either* that taking $1/2$ to be “small” is pushing things too far, or that lubrication theory is known to almost invariably give accurate results even when the “small parameters” are not actually very small. Undoubtedly (as in all lubrication theory analyses) there will be regions of the flow where lubrication theory is not valid (namely close to the limbus): here, as usual, we argue that the main details and topology of the flow do not depend on the behaviour in these regions.

One way in which this uncertainty may be permanently removed is to compare the results from lubrication theory to those generated by a fully numerical study. We carried out this programme of work using FEMLAB[®], a commercial finite-element equation solver, solving the full Navier–Stokes equations and corresponding complete coupled convection/diffusion problem. For each of the flows considered in Sections 2–5 above, the agreement between the full numerical calculations and the theory was remarkable. We now give an illustrative example: we calculated the flow and temperature profile for the buoyancy driven flow considered in Section 2, using standard values and a temperature difference of one degree.

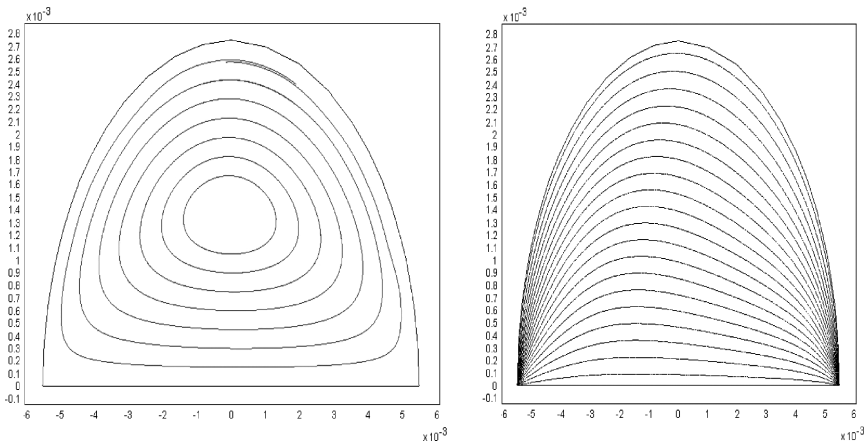


Fig. 8 Numerical flow streamlines (*left*) and temperature contours (*right*) for buoyancy-driven flow in the anterior chamber with a temperature difference of 1°C using standard parameter values. The calculations were performed using FEMLAB[®] with a mesh consisting of 2752 linear elements, giving a total of 18396 degrees of freedom.

Both streamlines and temperature contours are shown in Fig. 8: apart from the obvious qualitative agreement with our previous theoretical calculations, the results also show striking quantitative agreement. For example, for this flow the theory predicts that the maximum value of the horizontal speed u will be 0.1783 mm/s and will occur at the point $(0, 0.578 \times 10^{-3})$. The numerical calculations give these quantities as 0.1738 mm/s and $(0, 0.580 \times 10^{-3})$ respectively.

Likewise, FEMLAB[®] was used to perform three-dimensional phakodensitis calculations for the full Navier–Stokes equations. Once again, both the qualitative and quantitative agreement with the lubrication theory solutions was remarkable: for example, the theoretical value of the maximum horizontal speed on the z axis predicts that speed to be $1.002 \times 10^{-5}\text{ m/s}$ at $z = 1.375\text{ mm}$, whereas the numerical calculations (1888 elements, 10943 degrees of freedom) give values of $0.96 \times 10^{-5}\text{ m/s}$ and $z = 1.369\text{ mm}$ respectively.

7. Flow due to REM

It is now almost exactly 50 years since Rapid Eye Movement (REM) during sleep was discovered and reported in [Aserinsky and Kleitman \(1953\)](#). The phenomenon has attracted continuing interest from a wide range of scientific disciplines including ophthalmology, psychology, neurology and psychiatry and is familiar to members of the public with no scientific background, who usually believe either that the movement is associated with the subject “looking at what they are dreaming” or that its purpose is “hard disc defragmentation”—the brain sorts and reprocesses the information that has been gathered during the day. Though notoriously hard to assess experimentally, it appears that the balance of current scientific opinion favours the latter explanation (see, for example [Crick and Mitchison, 1983](#); [Hobson, 1990](#)).

Recently, however, a radical alternative explanation for REM sleep was advanced in Maurice (1998). Partly inspired by the observation that corneal vascularization was present in a patient who had suffered complete ptosis (eyelid droop) and loss of ocular motility, this relied on the fact that, during sleep, the buoyancy mechanisms that are normally responsible for stirring the aqueous humour in the anterior chamber (see Sections 2 and 4) are not present. It is also known (see, for example Maurice, 1967; Maurice, 1984) that the nutrients that are required to sustain the cornea cannot come from the limbus and must be carried to the posterior surface of the cornea by the aqueous. It was therefore suggested in Maurice (1998), that the purpose of REM might be to promote mixing in otherwise stagnant aqueous humour so that the oxygen supply to the cornea could be maintained.

In order to evaluate the mixing that may be produced by REM during sleep, it is necessary to understand the nature of REM. REM sleep is characterised by rapid (and typically jerky) movements of the eyes behind closed lids. These appear to take place in all directions and may involve single, disconnected movements or oscillatory motions. Periods of REM typically last initially for about 20 min, during which electroencephalographical information indicates a state close to arousal (see, for example Maurice, 1998). Periods of REM sleep become more prolonged as slumber continues; patients typically experience three or four periods of REM sleep during a night.

Aqueous mixing ascribed to REM has been reported in both humans (see Maurice, 1998) and rabbits (see Holm, 1968). The details of eye speed, position and rotation during REM were measured in Takahashi and Atsumi (1997), over a period of 40 nights' polysomnography performed on 20 healthy male patients. They reported a mean eyeball rotation speed of about 60°/s, which, with a typical mean sagittal diameter of 24 mm (see for example, Fatt and Weissman, 1992) corresponds to a linear speed of 0.0125 m/s. The number of eye movements averaged about 16 per min (one every 4 s) and the average distance of each movement was 6 degrees of rotation, corresponding to a distance of about 1.26 mm. The average time of movement was thus around 0.1 s, but is movement of this sort sufficient to cause the required amount of mixing? (Note that, compared to rapid types of eye movement during waking such as reading or saccadic motion where 20° movements can take place at 1000°/s (David et al., 1998), REM during sleep is a relatively sedate affair.)

Considered solely from a fluid mechanics viewpoint, the problem to be solved is to determine the flow that takes place when a closed container with boundary $\partial B = \{z = 0 \cup z = h(x, y)\}$ filled with fluid is subjected to a solid body translation $\mathbf{q}_s(t)$. We must therefore solve the Navier–Stokes equations

$$\mathbf{q}_t + (\mathbf{q} \cdot \nabla)\mathbf{q} = -\frac{1}{\rho}\nabla p + \nu\nabla^2\mathbf{q}, \quad \nabla \cdot \mathbf{q} = 0$$

with $\mathbf{q} = \mathbf{q}_s(t)$ on ∂B_t (where ∂B_t is the boundary of the moving anterior chamber) and $\mathbf{q}(x, 0) = \mathbf{q}_0(x)$. It is obvious, however, that one solution of this problem is given by

$$\mathbf{q} = \mathbf{q}_s(t), \quad p(r, t) = -\rho\mathbf{r} \cdot \mathbf{q}_s(t). \tag{21}$$

The fluid thus always moves simply as a solid body, and no mixing can ever take place, completely destroying the hypothesis advanced in Maurice (1998). Of course, it is not clear that (21) is the only solution to the problem. Indeed, intuition suggests that some mixing may occur if a closed container of fluid is translated fast enough. It is therefore tempting to try to analyse the linear stability of the solution (21). Unfortunately, this gives rise to a very awkward problem whose resolution is outside the scope of the current study. Essentially, we are required to determine the stability of a solution whose base flow is (a) unsteady and (b) takes place in a region which has a non-planar boundary. To give an idea of some idea of the difficulties involved, consider the stability problem for a steady rigid body translation base flow $\mathbf{q} = U_0 \hat{\mathbf{e}}_x$, $p = \text{constant}$. Proceeding in the normal way by linearising and eliminating the pressure, we find that the non-dimensional perturbation stream function $\hat{\psi}$ satisfies the equation

$$\hat{\nabla}^4 \hat{\psi} = Re \hat{\nabla}^2 (\hat{\psi}_t + \hat{\psi}_{\hat{x}})$$

(where $Re = LU_0/\nu$) with $\hat{\psi} = \hat{\psi}_n = 0$ on $\hat{z} = 0$ and $\hat{z} = \hat{h}(\hat{x})$. It is now possible to set $\hat{\psi} = \hat{\phi}(\hat{x}, \hat{z})e^{i\omega t}$ in the normal way to remove the time dependency, but the geometric dependence of the boundary conditions means that no Orr–Sommerfeld type ordinary differential equation may be derived, and a fully two-dimensional eigenvalue problem must be solved.

Since the stability problem for linear translation appears to be extremely difficult, we should ask if it is possible to invoke Navier–Stokes uniqueness theorems to determine whether or not rigid body motion is the only possible flow in a rigid sealed container. Unfortunately, such theory is not at all well-developed. The existence of weak solutions (i.e. solutions satisfying the weak form of the Navier–Stokes equations in an averaged function-theoretic sense) was proved over seventy years ago (Leray, 1934), but no real progress has since been made in proving weak uniqueness. For strong (i.e. smoother) solutions even less progress has been made (for a discussion of cases where the boundaries move, see Foias et al. 2000).

One final point should be made concerning rigid body motion of aqueous during REM: the simple “rigid body” solution given above is valid only for pure translation of the boundaries and evidently no longer applies when rotation is involved. To illustrate this, let us consider a flow region with a circular boundary and use cylindrical polar coordinates. Under pure translation (21) provides an exact “rigid body flow” solution to the Navier–Stokes equations. However, if the motion of the boundary is given by $\mathbf{q}_s = f(t)\hat{\mathbf{e}}_\theta$, then the “rigid body velocity” $\mathbf{q} = 0\hat{\mathbf{e}}_r + rf(t)\hat{\mathbf{e}}_\theta + 0\hat{\mathbf{e}}_z$ is *not* an exact solution of the Navier–Stokes equations.

Throughout this paper, we have ignored the curvature of the iris on the grounds that the anterior chamber is significantly smaller in height the radius of the eye. In the case of REM, to leading order the anterior chamber thus undergoes a purely translational movement. To next order, however, rotation (about the axis of the eye) is involved, centripetal accelerations and centrifugal forces can no longer be ignored, the rigid body motion discussed above is no longer an exact solution of the Navier–Stokes equations and mixing must occur. The resultant flow problem is, of course, unsteady and fully three-dimensional and its analysis appears to be possible only via a large-scale numerical study.

8. Conclusions

In this study simple fluid dynamical models have been posed for all of the mechanisms known to the authors that may cause the flow of aqueous in the anterior chamber. Each mechanism and the resulting flow has been analysed in isolation: however the linearity of the lubrication theory equations ensures that combinations of these flows may also be modelled and analysed if desired. Though the use of lubrication theory constitutes an approximation, its adoption is justified both by the parameter values involved and the agreement of the result with known data and estimates.

One of the key results of the work presented above is that the buoyancy induced by temperature gradients in the eye is by far the most pervasive mechanism for causing anterior chamber flow, producing velocities that are orders of magnitude greater than those due to any other physical mechanism. Though gravity and secretion of aqueous from the ciliary body can give rise to flows which may be important in the absence of temperature gradients, the role that buoyancy-driven flow has to play in influencing the formation of hyphemas, hypopyons and Krukenberg spindles is a dominant one.

Our analysis of phakododesis is necessarily more speculative since the complete absence of any experimental results concerning lens movement means that we have no information as to the strength of the flows that may be produced. If any experimental evidence should come to light, then a number of possibilities present themselves. An elastic model of the motion of the lenses suspended from the suspensory ligaments could be proposed, and since presumably the motion of the lenses is of relatively small magnitude it would be possible not only to attempt to calculate the vertical inlet speed $w_0(r, \theta, t)$ but also to use lubrication theory to couple the fluid motion to the flow behind the iris. In this way a very detailed model of phakododesis-driven flow in the anterior chamber could be studied.

Regarding the purpose of REM during sleep, the suggestion of [Maurice \(1998\)](#) is undoubtedly a highly controversial one. Indeed, in informal discussions with medical practitioners the authors have been unable to find any supporters of the idea that the evolutionary purpose of REM is to prevent corneal anoxia. From a fluid mechanics point of view, we have exhibited strong evidence that REM cannot produce aqueous mixing. It is only the lack of suitable uniqueness theorems for the Navier–Stokes equations that prevents this evidence from being decisive, and we have seen that the fluid mechanical stability problem that would settle the issue for certain is unfortunately a formidable technical challenge. On balance, however, it appears highly unlikely that REM can produce aqueous mixing and we must discount the proposals in [Maurice \(1998\)](#).

There may also be scope for considering flow that takes place not in, but in the vicinity of the anterior chamber. During the passage of flow of aqueous between the ciliary body and the canal of Schlemm, the aqueous exits the anterior chamber via the trabecular meshwork, which possesses no independent means of nourishment and thus relies on the aqueous humour to remain healthy. Studies of the manner in which aqueous passes from the anterior chamber into the canal of Schlemm, and how this affects aqueous facility have previously been carried

out (see, for example Allingham et al. (1992); Johnson et al. (1992); Ethier et al. (2004)). Further calculations based on Darcy's or Ergun's law (Ergun, 1952) could be carried out to determine (for example) what degree of blockage of the trabecular meshwork would be required to threaten the onset of elevated intraocular pressure. Finally, the ultrafiltration process that produces aqueous from blood is little understood. Modelling the flow produced by the ciliary body would undoubtedly be a valuable exercise.

Acknowledgements

The authors are indebted to Mr C.R. Canning of the Eye Unit, Southampton General Hospital, Tremona Road, Southampton, for providing encouragement, insight and understanding of the many components and functions of the eye.

References

- Abramowitz, M., Stegun, I.A. (Eds.) 1972. Handbook of Mathematical Functions. Dover, New York.
- Allingham, R.R., Dekater, A.W., Ethier, C.R., Anderson, P.J., Hertzmark, E., Epstein, D.L., 1992. The relationship between pore density and outflow facility in human eyes. *Inv. Ophthalm. Vis. Sci.* 33, 1661–1669.
- Aserinsky, E., Kleitman, N., 1953. Regularly occurring periods of eye motility, and concomitant phenomena, during sleep. *Science* 118, 273–274.
- Batchelor, G.K., 1985. An Introduction to Fluid Dynamics. Cambridge University Press, Cambridge, UK.
- Bron, A.J., Tripathi, R.C., Tripathi, B.J., 1997. Wolff's Anatomy of the Eye and Orbit, 8th edn. Chapman & Hall, London.
- Brubaker, R.F., 1996. Measurement of aqueous flow by fluorescein photometry. In: Ritch, R., Shields, M.B., Krupin, T. (Eds.), *The Glaucomas*. Mosby, St. Louis, MO.
- Crick, F., Mitchison, G., 1983. The function of dream sleep. *Nature* 304, 111–114.
- Canning, C.R., Greaney, M.J., Dewynne, J.N., Fitt, A.D., 2002. Fluid flow in the anterior chamber of the human eye. *IMA J. Math. Appl. Med. Biol.* 19, 31–60.
- David, T., Smye, S., Dabbs, T., James, T., 1998. A model for the fluid motion of vitreous humour of the human eye during saccadic motion. *Phys. Med. Biol.* 43, 1385–1399.
- Ergun, S., 1952. Flow through packed columns. *Chem. Eng. Prog.* 48, 89–94.
- Ethier, C.R., Johnson, M., Ruberti, J., 2004. Ocular biomechanics and biotransport. *Ann. Rev. Biomed. Eng.* 6, 249–73.
- Fatt, I., Weissman, B.A., 1992. *Physiology of the Eye*, 2nd edn. Butterworth, Heinmann, Boston.
- Foias, C., Manley, O., Rosa, R., Temam, R., 2000. *Navier–Stokes Equations and Turbulence*. Cambridge University Press, Cambridge, UK.
- Gerlach, J.C., Hentschel, F., Spatkowski, G., Zeilinger, K., Smith, M.D., Neuhaus, P., 1997. Cell detachment during sinusoidal reperfusion after liver preservation—An in vitro model. *Transplantation* 64, 907–912.
- Hobson, A., 1990. Ontogenetic development of the human sleep-dream cycle. *Neuroscience* 10, 371–382.
- Holm, O., 1968. A photogrammetric method for estimation of the pupillary aqueous flow in the living human eye. *Acta Ophthalmol.* 46, 254–283.
- Johnson, M., Shapiro, A., Ethier, C.R., Kamm, R.D., 1992. Modulation of outflow resistance by the pores of the inner wall endothelium. *Inv. Ophthalm. Vis. Sci.* 33, 1670–1675.
- Leray, J., 1934. Sur le mouvement d'un liquide visqueux emplissant l'espace. *Acta Math.* 63, 193–248.
- Maurice, D.M., 1967. Nutritional aspects of corneal grafts and prostheses. In: Rycroft, P. (Ed.), *Corneo-plastic Surgery*. Pergamon, Oxford.

- Maurice, D.M., 1984. The cornea and sclera. In: Davson, H. (Ed.), *The Eye*, Vol. 1B, 3rd edn. Academic Press, New York.
- Maurice, D.M., 1998. The Von Sallman Lecture 1996: An ophthalmological explanation of REM sleep. *Exp. Eye Res.* 66, 139–145.
- Takahashi, K., Atsumi, Y., 1997. Precise measurement of individual rapid eye movements in REM sleep of humans. *Sleep* 20, 743–752.
- Vankooten, T.G., Schakenraad, J.M., Vandermei, H.C., Dekker, A., Kirkpatrick, C.J., Busscher, H.J., 1994. Fluid shear-induced endothelial-cell detachment from glass—Influence of adhesion time and shear-stress. *Med. Eng. Phys.* 16, 506–512.
- Wyatt, H.J., 1996. Ocular pharmacokinetics and conventional flow. *J. Ocul. Pharmacol. Therapeut.* 12, 441–459.